Bioelectrochemistry 165 (2025) 108981

Contents lists available at ScienceDirect

Bioelectrochemistry

journal homepage: www.journals.elsevier.com/bioelectrochemistry

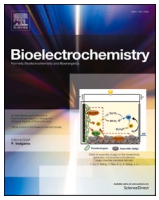

Electrochemical quantification of β-glucosidase activity for inhibitor screening applications☆

Catalina Farcas [a], C. Reyes Mateo [b], Francisco Montilla [a,*]

[a] Departamento de Química Física and Instituto Universitario de Materiales de Alicante (IUMA), Universidad de Alicante, Carretera San Vicente s/n, 03690 Alicante, Spain.
[b] Instituto de Investigación, Desarrollo e Innovación en Biotecnología Sanitaria de Elche (IDiBE), Universidad Miguel Hernández, Avenida de la Universidad s/n, 03202, Elche, Alicante, Spain

ARTICLE INFO

Keywords:
Electrochemical biosensor
B-Glucosidase
P-Arbutin
Voltammetric detection
Acarbose
Enzyme inhibition

ABSTRACT

The measurement of enzymatic activity of glucosidases is essential for its use in various clinical and industrial applications. Inhibitors of these enzymes are promising candidates as antidiabetic drug. This study presents the development of an electrochemical device for quantifying β-glucosidase activity using an electrochemical transduction method. Enzyme activity was evaluated in a citrate buffer solution with *p*-arbutin (hydroquinone-β-D-glucopyranoside) as the substrate, employed for the first time in this context. The enzymatic hydrolysis of the glycosidic bond produced hydroquinone, which was quantified via voltammetric measurements to determine the hydrolysis rate. To develop a device for the screening of inhibitory effects on glucosidase, this enzyme was immobilized into silica matrix and its activity was evaluated. Entrapped enzyme shows partial retention of its catalytic function that can be measured by means of the electrochemical transduction. The inhibitory effects of various sugars and acarbose (a commonly used antidiabetic drug) were investigated using the sensor with the immobilized enzyme. Inhibition rates detected ranged from 87 % to 13 % for the sugars and 17 % for acarbose.

1. Introduction

Glucosidases are a class of enzymes that play a crucial role in the hydrolysis of glycosidic bonds, which link carbohydrates to other molecules. Specifically, β-glucosidases, (BGL) catalyses the breakdown of β-glycosidic bonds, releasing glucose and other molecules. This process is vital in various biological and industrial contexts [1,2]. In food and beverage industry, BGL are used to improve flavours by releasing simple sugars from glycosidic precursors [3,4]. In cellulose degradation, which is particularly crucial for biofuel production, it participates by converting lignocellulosic biomass into fermentable sugars for ethanol production. Finally, in agriculture, BGL enhances the decomposition of plant residues in the soil, thus contributing to nutrient cycling [5–8].

BGL in humans are vital for glycolipid metabolism, and their activity levels are crucial to diagnose and understand various diseases. For example, serum BGL activity provides predictive values for early diagnosis for neonatal necrotizing enterocolitis and Gaucher disease [9] and the gut microbial enzyme BGL can be used like a biomarker for the early detection and monitoring of polycystic ovarian syndrome in women with metabolic disorders [10].

The activity of BGL enzyme can be determined using several methods like fluorescence spectroscopy [11–13], colorimetry [14], chromatography [15], agar plate-based assays [16] or mediated cascade reaction through glucose measurement [17].

There are some reports in the scientific literature that describe devices to measure glucosidase activity using electrochemical transduction [18]. Electrochemical transduction is particularly well-suited for sensor development due to its high sensitivity, fast response times, and relatively low cost. However, the literature published on this topic commonly relies on the formation of nitrophenol as the basis for electrochemical detection [19]. While nitrophenols are particularly adequate for the optical transduction (due to its yellow colour as well as its fluorescence quenching ability), these species are not easily detectable with conventional electrodes. For that reason, it is necessary to perform complex surface modifications to improve electrode performance and enhance detection sensitivity [20].

We propose the use of arbutin (4-Hydroxyphenyl-β-D-glucopyranoside) as substrate for BGL. Arbutin is a naturally occurring glycoside

☆ This article is part of a Special issue entitled: 'BES 2024' published in Bioelectrochemistry.

* Corresponding author.
E-mail address: francisco.montilla@ua.es (F. Montilla).

https://doi.org/10.1016/j.bioelechem.2025.108981
Received 21 November 2024; Received in revised form 20 February 2025; Accepted 29 March 2025
Available online 4 April 2025

found in plants (like bearberry, cranberry, and blueberry) employed in cosmetics for its skin-brightening properties [21]. The hydrolysis of arbutin would drive to the delivery of glucose and hydroquinone (see Scheme 1), being the last product a typical redox probe that can be detected by electrochemical methods with conventional surfaces, as carbon screen-printed electrodes.

The ability to measure BGL activity provides a suitable platform for the discovery of inhibitors of this enzyme that are highly valuable for developing new treatments for diseases like diabetes, cancer, and viral infections, while also enhancing biofuel production and biotechnological processes [19,22]. Some of the glucosidase inhibitors studied until now include therapeutical drugs like Kojibiose (for the treatment of HIV infections), Nojirimycin (inhibiting both alpha- and beta-glucosidase), acarbose, isofagomine, miglitol, and voglibose among others [13,23–26].

In the present work we propose an electrochemical device for the measurement of the activity of BGL enzyme making use of an electrochemical transduction method, employing arbutin as enzymatic substrate. To develop the device, the enzyme was entrapped into silica matrix, deposited over screen printed electrodes and determined its apparent activity. Using this device, we assessed the inhibitory effects of a range of molecules, including D(+)glucose, L(−)glucose, D(−)fructose, D(+)galactose, sucrose, gluconolactone, and L(−)xylose, as well as the antidiabetic medication, acarbose. This electrochemical device serves as a versatile platform for screening potential BGL inhibitors, opening avenues for applications in medicine and biotechnology and supporting new strategies for inhibitor-based therapies.

2. Experimental part

β-Glucosidase from almonds (lyophilized powder, ≥4 units/mg, molecular weight 135 kDa), *p*-arbutin (≥98 %), D(+)glucose, L(−) glucose, D(−)fructose, D(+)galactose, sucrose, gluconolactone, L(−) xylose, tetraethyl orthosilicate (≥98.0 %) were purchased from Sigma-Aldrich. Citric acid monohydrate and sodium citrate dihydrate were purchased from Fisher and Acarbose from Thermo Scientific. The 0.1 M citrate buffer solution was prepared using ultrapure water (18 MΩ cm, Merck Millipore® Milli-Q® water, Spain), the pH was adjusted to 5 by adding sodium hydroxide (purchased from Merck).

Electrochemical measurements were carried out in an EDAQ Potentiostat (ED410 model) connected to a function generator (EG&G Parc model 175). Metrohm DropSens Screen-Printed Carbon Electrode (SPE, Ref: DRP-C11L) was used for electrochemical measurements. The working and auxiliary electrodes were made of carbon (geometric area of the working electrode 0.126 cm^2) and the reference electrode was silver/silver chloride.

Fluorescence spectra and steady-state fluorescence anisotropy measurements were performed in a PTI QuantaMaster spectrofluorometeter (model QM-62003SE) equipped with excitation and emission polarizers. For the steady-state anisotropy determination, the corresponding vertically polarized and horizontally polarized emission intensities elicited by vertically polarized excitation (I_{VV} and I_{VH}, respectively) were determined. The degree of polarization or anisotropy (r) can be calculated from Eq. 1:

$$r = \frac{I_{VV} - GI_{VH}}{I_{VV} - 2GI_{VH}} \quad (1)$$

being G a correction factor related to the experimental setup. The G-factor accounts for the differential polarization sensitivity and was determined by measuring the polarized components of fluorescence of the sample with horizontally polarized excitation.

For the development of the electrochemical device, the enzyme BGL was immobilized in a silica sol-gel matrix. The silica-gel matrix was synthesized using the following procedure: First, 6 mL TEOS and 6 mL HCl 0.01 M was magnetically stirred for two hours in a closed vial. Then, the ethanol released during the hydrolysis was removed with a rotary evaporator (Heidolph laborota 4000 efficient) to avoid denaturation of the enzyme incorporated in the second step.

The enzyme was entrapped within a silica matrix monolith by mixing 1.1 mL colloidal sol and 1.1 mL of 100 mM phosphate buffer solution at pH 7.4, containing the enzyme, prepared directly in a conventional quartz optical cuvette. The solution gelled within 1 min, conforming to the shape of the cuvette. The immobilization of the enzyme BGL on SPE was carried out mixing 100 mM phosphate buffer solution at pH 7.4 containing the enzyme with the colloidal sol in a 1:1 volume ratio. A 5 μL-drop was then deposited on the surface of the working electrode. The gel was formed instantly, then washed several times with 100 mM citrate buffer at pH 5. Prior to its use, a drop of 100 μL of this buffer is deposited on top of the silica matrix formed, then the cyclic voltammograms were performed between −0.26 and 0.23 V to stabilize the BGL@Silica electrodes.

3. Results and discussion

3.1. Enzyme activity in solution

We performed a fluorescence spectroscopy study, since BGL is intrinsically fluorescent due to the presence of aromatic amino acids (mainly tryptophan and tyrosine residues), to determine an appropriate protein concentration to be used in the determination of the enzyme activity [27,28]. For this purpose, solutions with increasing concentrations of BGL were prepared and the emission spectra were collected, as shown in Fig. 1.

As expected, the fluorescence intensity increases as a function of the concentration. When plotting the maximum emission intensity versus concentration (inset of Fig. 1), a linear growth is observed below 10 μM of BGL. Above that concentration linearity is lost due to formation of protein aggregates [29].

Fig. 2.A shows the successive voltammogram of a carbon SPE containing a 105-μL drop of solution of BGL (10 μM, 1.4 mg/mL) in 0.1 M citrate buffer + arbutin (10 mM). In previous experiments (see Fig. S1 in the Supporting information), we checked that arbutin shows no intrinsic electrochemical response and does not suffer spontaneous hydrolysis in absence of BGL.

During the first voltammetric scan, no significant electrochemical process can be observed. After few voltammetric cycles oxidation and

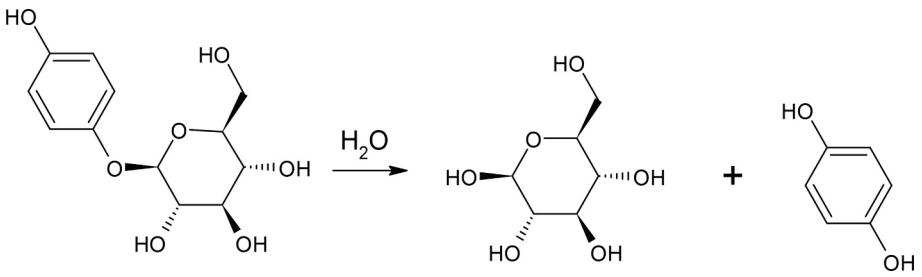

Scheme 1. Hydrolysis reaction of *p*-Arbutin

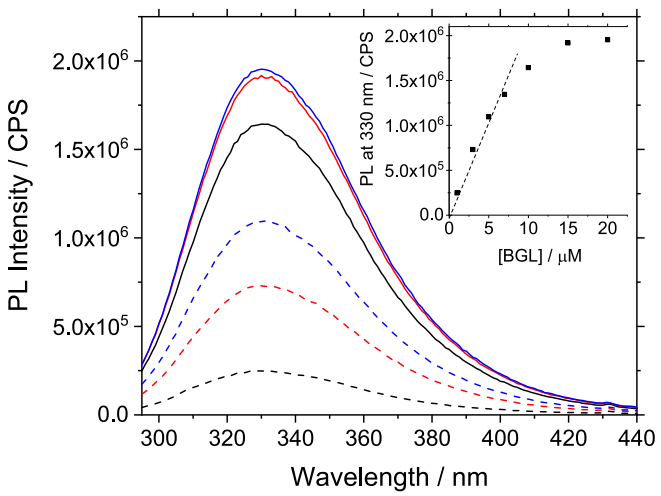

Fig. 1. Fluorescence emission spectra (λ_{exc} = 285 nm) of BGL in 0.1 M citrate buffer solution pH 5 at different concentration (dashed lines: back 1 μM; red 2 μM, blue 5 μM; solid lines: black 10 μM, red 15 μM, blue 20 μM). Inset: Variation of emission intensity at 330 nm. (For interpretation of the references to colour in this figure legend, the reader is referred to the web version of this article.)

reduction peaks emerge at 0.38 V and – 0.32 V. These peaks are clearly observable from the 3rd voltammetric cycle (1 min after the start of the experiment). The positive peak is related to the oxidation of hydroquinone to benzoquinone in the forward scan and the corresponding counterprocess appears in the backward scan. This hydroquinone is the product released to the solution due to the hydrolysis of arbutin catalysed by BGL (the electrochemical response of hydroquinone in this solvent can be observed in Fig. S2 of the Supporting information). These redox peaks continue growing during the experiment presented. The current density measured on the oxidation peak can be used to quantify the amount of hydroquinone released during the enzymatic reaction. Fig. 2.B shows the evolution of the concentration of HQ (hydroquinone) in the solution over time. In the time range of the experiment performed, a linear growth of the concentration of the product was observed, corresponding to pseudo-zero order kinetics, usually observed when the concentration of the substrate is much higher than that of the enzyme. The hydrolysis rate of arbutin was determined from the slope of this representation, being 0.153 mM/min.

3.2. Entrapment of the enzyme in silica. Spectroscopic characterization

Immobilized enzymes typically exhibit more thermal resistance and operational stability than their soluble form, so after testing the suitability of the substrate arbutin in electrochemical measurements, the next step to develop the electrochemical sensor was the immobilization of BGL on a silica matrix and the characterization of its properties. To determine the integrity of the encapsulated enzyme, a fluorescence study in different conditions was carried out to assess the enzyme stability under our working conditions.

Fig. 3 compares the fluorescence spectrum of the enzyme in solution (citrate buffer) and encapsulated within a silica hydrogel monolith, with the same concentration of enzyme in both cases.

A higher intensity of the emission spectrum of encapsulated enzyme was observed compared to the free one, which indicates that confinement induces a slight increase in the emission intensity of the fluorophores (mostly tryptophan) of the enzyme. The emission spectrum in solution shows a maximum at 331 nm (spectral centre of mass at 342.9 nm). The maximum of the emission of the enzyme in silica matrix appears slightly blue shifted with respect to that in solution (maximum at 329 nm, centre of mass at 341.6 nm) indicating that the environment is less polar for the encapsulated enzyme. These results suggest that the encapsulation process does not induce any denaturation in the protein (loss of specific tertiary structure), since in that case the tryptophan residues would be more exposed to the solvent and, consequently, the spectrum would be shifted towards higher wavelengths.

To gain insight into the mobility of the encapsulated enzyme, its fluorescence anisotropy was determined both, free in solution and after being immobilized in the gel matrix, excitation being performed at a wavelength of 285 nm. The fluorescence anisotropy for the BGL in solution was $r = 0.08$, indicating a high depolarized emission coming from the rotational free diffusion of the enzyme in the solution. When incorporated in the silica matrix the anisotropy rises to $r = 0.16$, suggesting that BGL diffusion is hindered probably due to its partial absorption on the silica pores that restricted its movement. Using the equation of Perrin equation (Eq. 2) the rotational diffusion coefficient of the enzyme can be estimated.

$$\frac{r_0}{r} = 1 + \frac{\tau}{\theta} = 1 + 6D\tau \tag{2}$$

Where r is the anisotropy, r_o is the fundamental anisotropy (anisotropy in absence of diffusion, with a value of 0.29 [30]), τ is the fluorescence lifetime of the fluorophore, θ is the rotational correlation time and D is the rotational diffusion coefficient. Considering that the fluorescence lifetime is the same for both cases, the apparent rotational

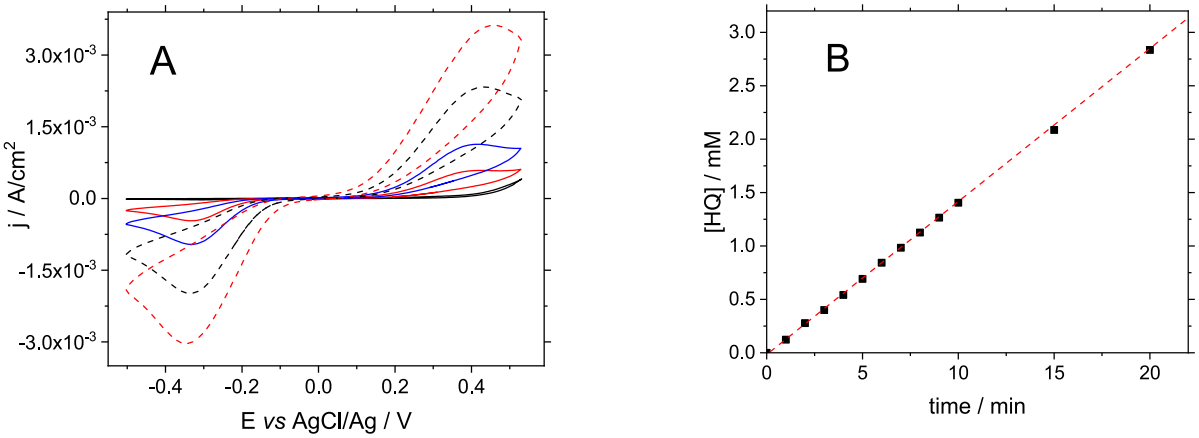

Fig. 2. **(A)** Cyclic voltammograms of SPE carbon electrode in a solution of 1.4 mg/mL BGL, 10 mM p-arbutin in 0.1 M citrate buffer (pH = 5). Scan rate 100 mV s^{-1}. Solid lines: Black 1st scan, red 30th cycle, blue 60th cycle; dashed lines: Back 120th cycle, red 180th cycle. **(B)** Evolution of the concentration of hydroquinone product formation over time for a solution with 1.4 mg/mL BGL+ 10 mM p-arbutin in 0.1 M citrate buffer (pH = 5).

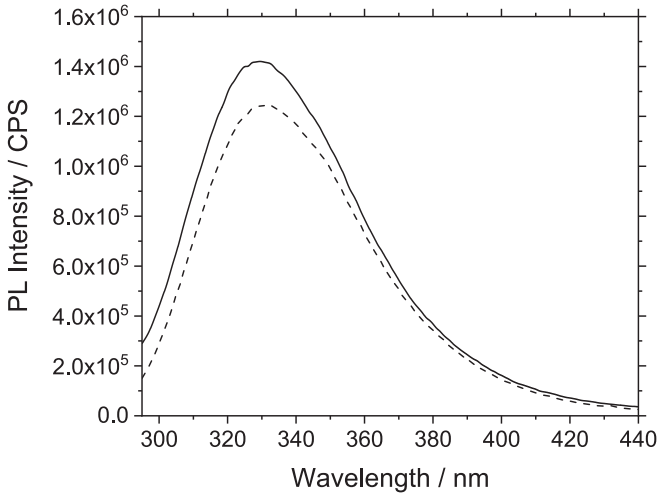

Fig. 3. Fluorescence emission spectra (λ_{exc} = 285 nm) of BGL (1.4 mg/mL) in solution (dashed line) and encapsulated in silica (solid line).

diffusion coefficient was found to be 3.3 times higher in solution compared to the silica matrix. This difference suggests that the sol-gel environment imposes constraints that limit the degrees of freedom of the protein, probably reducing the mobility and rotational amplitude of tryptophan residues. Consequently, the higher mobility and internal flexibility of the enzyme in solution will allow it to adopt more conformational states and interact more freely with substrates or other molecules, whereas the sol-gel matrix will restrict these movements, which may affect the catalytic efficiency of the enzyme and its interaction with substrates.

3.3. Enzyme activity entrapped in silica matrix

The enzymatic activity of BGL was studied after its incorporation within silica matrix. First, the carbon working electrode was modified with the 5 μL of the silica gel containing BGL. We studied the effect of the enzyme concentration encapsulated within the silica gel. First, we check the activity of the enzyme encapsulated in a silica droplet with the same concentration in the gel than in solution (1.4 mg/mL in the 5 μL of the silica, BGL-1.4@Silica) and deposited on the working electrode. Then, the electrode was rinsed with citrate buffer to remove the unreacted silica precursors. Finally, a 100-μL drop containing 0.1 M citrate buffer at pH 5 + 10 mM arbutin was added over the modified electrode. Fig. 4. A shows the cyclic voltammograms of the BGL-1.4@Silica electrode during this test.

The cyclic voltammogram of the silica modified electrode presents a significant increase of the current related to the double-layer charge (observed in the first scan), which is characteristic of silica modified SPE electrodes [31]. Initially no faradic peaks are observed because of the lack of electroactivity of the substrate. After 3 voltametric cycles oxidation and reduction peak emerges due to the formation of HQ by the hydrolysis of the substrate. These peaks are clearly visible from the 6th cycle. A continuous growth of the intensity is observed in the successive cycles, evidencing the progression of the enzymatic reaction. The current intensity of the oxidation peak can be related to the concentration of hydroquinone in the solution (Fig. S3 in the Supporting Information shows the electrochemical response of HQ solution with silica modified SPE).

Fig. 4.B shows the evolution of the concentration of the product detected voltammetrically during the experiment for the BGL-1.4@Silica electrode. Initially we observe that HQ concentration grows linearly –pseudo-zero order rate– up to 8 min of experiment (a concentration of HQ of 0.35 mM is reached). From the slope of this plot, we can determine a hydrolysis rate for arbutin of 0.053 mM/min. We denominated that period as high-rate regime (HRR). Following this pseudo-zero order period, a reduction in the slope is observed, reaching a lower hydrolysis rate of 0.0135 mM/min. We denominated that period as low-rate regime (LRR).

It is necessary to remark that these voltammetric experiments allow to determine only the apparent activity of the enzyme encapsulated in silica. The following factors affect the measurement of the real enzymatic activity in this system: (i) reduced accessibility of the substrate to reach the active site of the enzyme encapsulated in silica (ii) reduced accessibility of the products generated in hydrolysis also impedes diffusion to the electrode surface [31]; (iii) restricted mobility of the enzyme within the silica. The above-mentioned factors will drive to a lower measured activity of the encapsulated enzyme compared with the real activity.

The different slopes observed could be related with the accessibility of the substrate to different populations of encapsulated enzyme [31]. Initially, faster reaction is observed due to the presence of enzyme in more accessible sites (i.e. open pores or external sites). After the initial

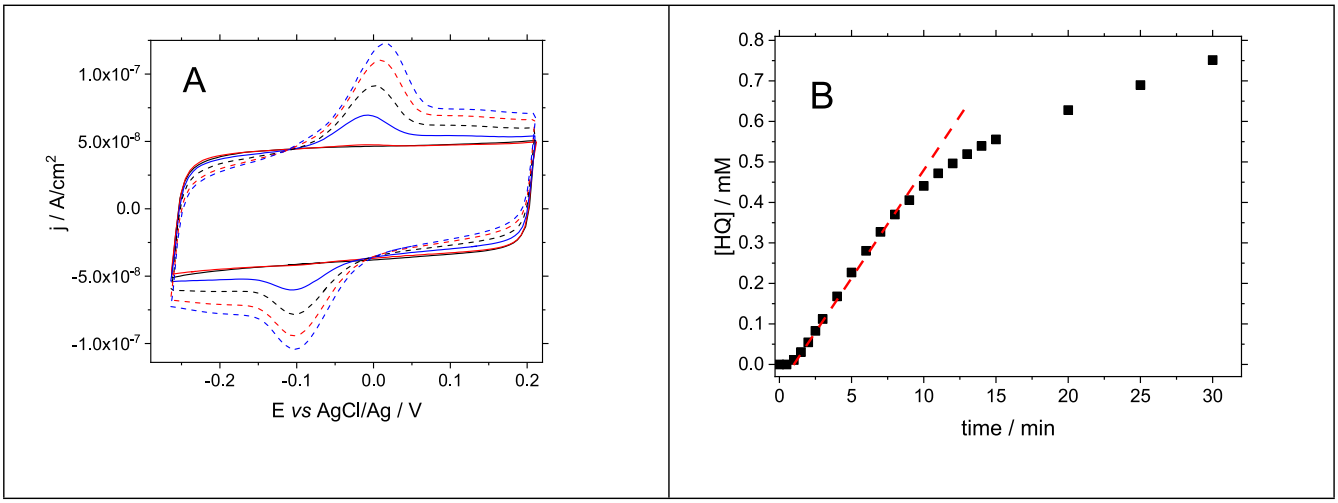

Fig. 4. (A) Cyclic voltammogram of BGL-1.4@Silica modified electrode in 10 mM arbutin in 0.1 M citrate buffer (pH = 5) at 100 mV s^{-1}. Solid lines: Black 1st scan, red 6th cycle, blue 30th cycle; dashed lines: Black 60th cycle, red 90th cycle, blue 180th cycle **(B)** Evolution of concentration of hydroquinone over time for the BGL-1.4@Silica electrode, 10 mM arbutin in 0.1 M citrate buffer (pH = 5). (For interpretation of the references to colour in this figure legend, the reader is referred to the web version of this article.)

period of fast hydrolysis, the enzyme in inner places within silica, presents a lower activity (low-rate regime, LRR), probably due to low accessibility of the substrate to the reaction centres. As previously indicated, the anisotropy measurement support this effect, as the lowering of the rotational diffusion coefficient of the enzyme in the silica matrix due to restricted mobility, parallels similar findings in other hydrolases incorporated within silica matrix [32,33], suggesting that while silica encapsulation enhances stability, it also reduces the enzyme's conformational flexibility, which could influence its catalytic efficiency and substrate interaction capabilities.

The decrease in the hydrolysis rate (the transition from HRR to LRR) can be also related to an inactivation process due to the accumulation of the hydrolysis products formed within the silica in close vicinity with the enzyme. One of the products of the arbutin hydrolysis (glucose) acts as BGL inhibitor (see following section). The accumulation of glucose confined in the gel may contribute to a progressive decrease in hydrolysis rate.

We performed experiments at increasing enzyme concentration within the silica droplet. Fig. 5 shows similar experiments for the concentration of 1.4, 7.0, 28 and 56 mg/mL of BGL in the silica droplet (see Fig. S4 for the voltammetric measurements of BGL-28@Silica).

In all the cases we observe an initial pseudo-zero order growth of HQ concentration (HRR regime) for times up to 6–8 min of experiment. The hydrolysis rate in the HRR regime increases as a function of the concentration of BGL confined in silica. It is remarkable that the rate for 28 mg/mL in silica reaches a hydrolysis rate near four times higher than in solution. Notably, further increases of the enzyme concentration up to 56 mg/mL within the silica droplet do not increases the hydrolysis rate, a saturation effect that can be related to the enzyme aggregation at such high concentration.

The following study was conducted using a BGL concentration of 28 mg/mL in silica, as this value offers an optimal balance between achieving a rapid and strong response while minimizing enzyme consumption.

3.4. Inhibition studies

Making use of the electrochemical device developed for the study of the apparent activity of the enzyme, we explored the inhibitory effect of different species on BGL. We checked different sugars, recognised as inhibitors of glucosidases [34] and an oligosaccharide (acarbose) that is used as anti-diabetic drug [35].

For inhibition studies the BGL@Silica-modified electrode was immersed in a solution containing 0.1 mM of sugar and left to incubate. The solution was then removed, and the electrode ensemble was rinsed with citrate buffer. Finally, a 100 μL-drop containing the substrate (10 mM arbutin in citrate buffer) was dispensed over the electrode, as in previous experiments, to measure the apparent activity of the enzyme.

Different incubation periods were checked to detect the inhibitors. No clear inhibitory effects were observed when the electrode is exposed to the solutions containing potential inhibitors for periods lower than 1 h (see Fig. S5 in the Supporting information). It may indicate that the presence of silica pores impedes the access of some of the sugars within the silica pores containing the encapsulated enzyme, and the rinsing step remove from the electrode all the potential inhibitors. Only a clear inhibitory effect is observed for gluconolactone, which can be attributed to its ability to bind to the active site of β-glucosidase. Gluconolactone adopts a distorted half-chair conformation that closely mimics the carbonium ion intermediate, a critical transition state in the enzyme's catalytic mechanism [36]. This structural similarity allows gluconolactone to act as a transition state analogue, quickly forming a temporary complex with the enzyme in the initial fast-binding step. This complex then becomes more tightly bound in the slower second step, effectively blocking enzyme activity from the very first minute. In contrast the rest of the sugars show a delayed inhibitory effect, as their lower affinity for the active site requires more time to compete with the natural substrate and accumulate around the enzyme, resulting in noticeable inhibition only after approximately four minutes [36,37].

Experiments performed with longer incubation period (24 h-incubation) followed by the rinsing step are displayed in Fig. 6. This figure shows the evolution of the hydroquinone concentration formed during the hydrolysis reaction for the sensors after its exposition to glucose, xylose, gluconolactone and without inhibitor (the experiments with the rest of inhibitors are presented in the Fig. S6 of the Supporting information).

It is remarkable to check that most of the inhibitors assayed present a

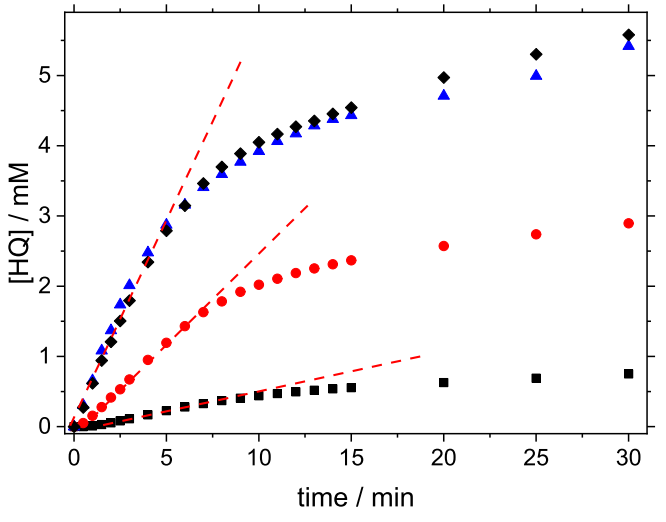

Fig. 5. Evolution of the concentration of hydroquinone formation for the different BGL@Silica modified electrodes. Enzyme concentration within silica: 1.4 mg/mL (BGL-1.4@Silica, black squares), 7.0 mg/mL (BGL-7.0@Silica, red circles), 28 mg/mL (BGL-28@Silica, blue triangles), 56 mg/mL (BGL-56@Silica, black rhombus). Experiment conditions as in Fig. 4: 10 mM p-arbutin in 0.1 M citrate buffer (pH = 5). (For interpretation of the references to colour in this figure legend, the reader is referred to the web version of this article.)

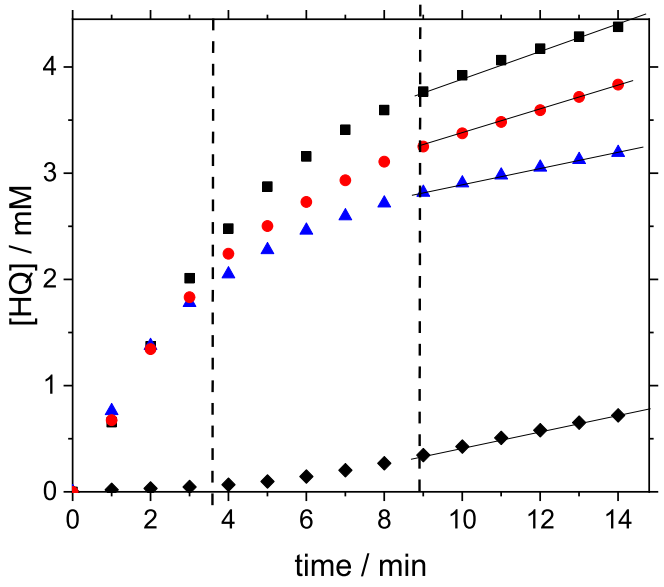

Fig. 6. Concentration of product (HQ) formed as a function of time for BGL@Silica electrode in a solution containing 10 mM *p*-arbutin in 0.1 M citrate buffer at pH 5 in: absence of inhibitor (black squares) and after exposition to 0.1 M of D(+)-glucose (red circles), L(−) xylose (blue triangles) and gluconolactone (black rhombus). (For interpretation of the references to colour in this figure legend, the reader is referred to the web version of this article.)

similar qualitative behaviour. The initial high-rate regime (HRR) of the enzyme is nearly unaffected by the presence of the inhibitor and the rate of formation of product is similar in all the experiments, indicating that the rinsing step easily remove the inhibitors residing in open or accessible pores of silica. Notably, low HRR value is still observed in the experiments after exposition to gluconolactone (HRR 0.016 mM/min), due to the ability of this compound to tightly bind on BGL [36]. The rest of the inhibitors tested present a competitive-inhibition mechanisms [34,38] and the value of HRR rate is similar in all the cases, around 0.7 mM/min (see Table S1 in the Supporting Information).

The major differences in the enzyme activity are observed for times of experiments higher than 8 min, corresponding to the LRR zone. It may indicate that the rinsing steps easily remove the inhibitor on the accessible enzymes within silica (outer sites) but inhibitors are still retained in less accessible pores. Most values in the LRR zone were found to be 5 to 9 times smaller than HRR values, with sucrose showing the most substantial decrease, having an LRR rate of 0.029 mM/min—26 times smaller than its HRR (see Table S1 in Supporting Information).

To determine the optimal time to detect the inhibitory effect, we determined the amount of HQ formed in the experiments performed in presence of inhibitors $-[HQ]_{inh}(t)-$ and we compared with the amount obtained in experiments in blank solutions (in absence of inhibitor) $-[HQ]_0(t)-$. The resulting difference is referred to as the Inhibition-adjusted Product Yield: $IPY(t) = [HQ]_0(t)-[HQ]_{inh}(t)$. Fig. 7.A shows *IPY* for D(+) glucose, D(−) fructose, L(−) xylose, and acarbose.

Notably, different *IPY* becomes clearly detectable from 3 to 4 min for all sugars tested, and after approximately 12 min, this yield tends to stabilize across all inhibitors, suggesting that the device can reliably assess inhibition by measuring within this period. The values of *IPY* can be related to partial inactivation of the enzyme present within the devices. To quantify the amount of active enzyme that is apparently active after its exposure to the inhibitor, we determined the Active Enzyme Ratio (*AER*) using eq. 3:

$$AER(t) = \frac{IPY\ (t)}{[HQ]_0(t)} \tag{3}$$

This value was calculated for an interval between 12 and 15 min, corresponding to the stabilization of this parameter and its mean value, along with the standard deviation, is represented in Fig. 7.B. Our findings on the inhibitory effects of gluconolactone and D(+) galactose align closely with those reported by Tanaka et al. [36], where gluconolactone exhibited the strongest inhibition. Consistently, in our study, gluconolactone reduced BGL activity to just 13 %, while D(+) galactose showed notably weaker inhibition, supporting Tanaka et al.'s findings on its lower enzyme affinity. In comparison, the remaining sugars maintained between 77 % and 87 % BGL activity, demonstrating a broader inhibitory profile across sugars tested.

4. Conclusions

This study successfully demonstrates the development and application of an electrochemical device for the quantification of β-glucosidase (BGL) enzyme apparent activity using an electrochemical transduction method. The use of arbutin as a suitable substrate for this enzyme is shown for the first time. This compound has not electrochemical activity, as measured by conventional Carbon Screen-printed electrodes, however the enzyme is able to hydrolyse this compound forming electroactive hydroquinone. The rate of product formation can be followed by voltametric measurements allowing to determine the activity of the enzyme in solution and incorporated in silica matrix. After the immobilization in silica the enzyme partially retains its catalytic function, but a loss of activity after 6–8 min is detected. Notably, during the initial stages of the reaction, the enzyme exhibited higher apparent activity when immobilized on the silica matrix compared to its activity in solution.

The inhibitory effects of different sugars, gluconolactone and acarbose on BGL activity were also investigated. The evaluation of BGL immobilized on a silica matrix revealed that the different sugars tested, along with acarbose, exhibited inhibition rates that ranged from 13 % to 87 %.

The identification of BGL inhibitors like acarbose highlights their potential for advancing medical treatments, understanding disease mechanisms, and contributing to biotechnological applications. These findings underscore the importance of developing novel inhibitors for therapeutic purposes and scientific research. The results suggest that further exploration of BGL inhibitors could lead to innovative therapies for various diseases and enhance the utility of electrochemical devices in scientific and industrial settings.

CRediT authorship contribution statement

Catalina Farcas: Writing – review & editing, Writing – original draft, Methodology, Investigation, Formal analysis. **C. Reyes Mateo:** Writing – review & editing, Validation, Methodology, Funding

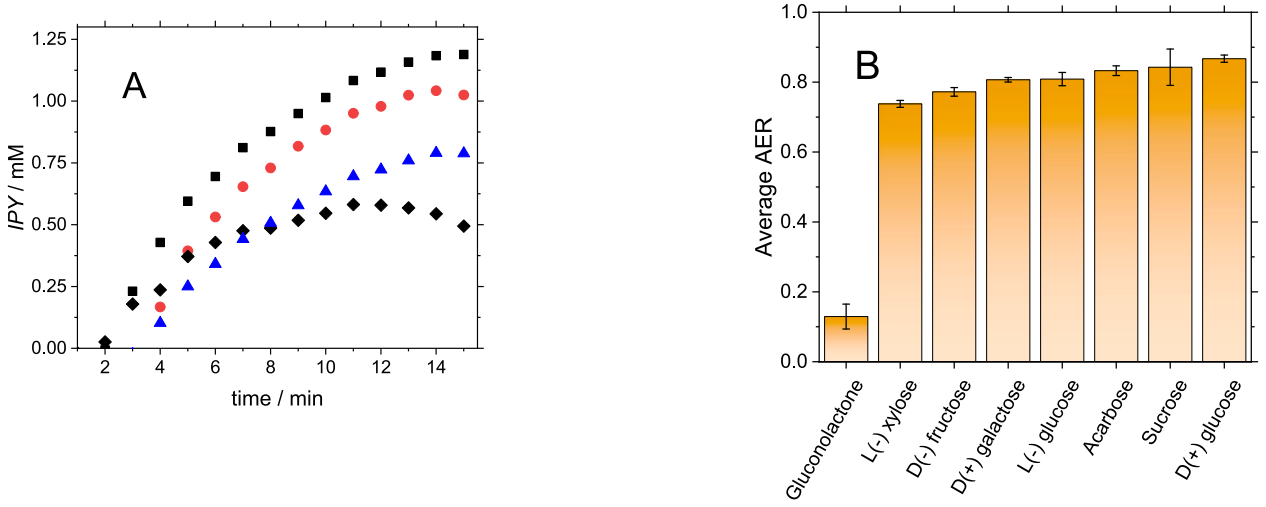

Fig. 7. (A) *IPY* as a function of time for BGL@Silica electrode in a solution containing 10 mM *p*-arbutin, 0.1 M citrate buffer at pH 5 after exposure to different inhibitors: L-xylose (black squares), D-fructose (red circles), Acarbose (blue triangles) and D-glucose (black rhombus). (B) Average *AER* for BGL@Silica electrode in a solution containing 10 mM *p*-arbutin, 0.1 M citrate buffer at pH 5 after exposure to different inhibitors. (For interpretation of the references to colour in this figure legend, the reader is referred to the web version of this article.)

acquisition, Formal analysis, Data curation, Conceptualization. **Francisco Montilla:** Writing – review & editing, Validation, Supervision, Methodology, Funding acquisition, Formal analysis, Data curation, Conceptualization.

Declaration of competing interest

The authors declare that they have no known competing financial interests or personal relationships that could have appeared to influence the work reported in this paper.

Acknowledgments

Financial support by Spanish Ministry of Science (TED2021-129894B-I00 and PID2022-138507OB-I00 projects), Generalitat Valenciana (MFA/2022/058 project) and European Union (NextGeneration EU PRTR-C17·I1) is gratefully acknowledged.

Appendix A. Supplementary data

Supplementary data to this article can be found online at https://doi.org/10.1016/j.bioelechem.2025.108981.

Data availability

Data will be made available on request.

References

[1] P. Kannan, M. Shafreen, M.A.B. Achudhan, A. Gupta, L.M. Saleena, A review on applications of β-glucosidase in food, brewery, pharmaceutical and cosmetic industries, Carbohydr. Res. 530 (2023) 108855, https://doi.org/10.1016/j.carres.2023.108855.
[2] G. Singh, A.K. Verma, V. Kumar, Catalytic properties, functional attributes and industrial applications of β-glucosidases, 3, Biotech 6 (2016) 1–14, https://doi.org/10.1007/s13205-015-0328-z.
[3] F.M.R. Graf, M. Buchhaupt, Comparative investigations on different β-glucosidase surrogate substrates, Fermentation 8 (2022) 1–9, https://doi.org/10.3390/fermentation8020083.
[4] G. Lomolino, F. Zocca, P. Spettoli, A. Lante, Detection of β-glucosidase and esterase activities in wild yeast in a distillery environment, J. Inst. Brew. 112 (2006) 97–100, https://doi.org/10.1002/j.2050-0416.2006.tb00237.x.
[5] S. Ariaeenejad, S. Nooshi-Nedamani, M. Rahban, K. Kavousi, A.G. Pirbalooti, S. S. Mirghaderi, M. Mohammadi, M. Mirzaei, G.H. Salekdeh, A novel high glucose-tolerant β-glucosidase: targeted computational approach for metagenomic screening, front. Bioeng, Biotechnol 8 (2020) 1–14, https://doi.org/10.3389/fbioe.2020.00813.
[6] C. Huang, Y. Feng, G. Patel, X. Qian Xu, J. Qian, Q. Liu, G. Yin Kai, Production, immobilization and characterization of beta-glucosidase for application in cellulose degradation from a novel aspergillus versicolor, Int. J. Biol. Macromol. 177 (2021) 437–446, https://doi.org/10.1016/j.ijbiomac.2021.02.154.
[7] A.T. Adetunji, F.B. Lewu, R. Mulidzi, B. Ncube, The biological activities of β-glucosidase, phosphatase and urease as soil quality indicators: a review, J. Soil Sci. Plant Nutr. 17 (2017) 794–807, https://doi.org/10.4067/S0718-95162017000300018.
[8] V. Venezia, F. Sannino, A. Costantini, B. Silvestri, S. Cimino, V. Califano, Mesoporous silica nanoparticles for β-glucosidase immobilization by templating with a green material: tannic acid, Microporous Mesoporous Mater. 302 (2020) 110203, https://doi.org/10.1016/j.micromeso.2020.110203.
[9] J.L. Gómez-Chaparro Moreno, A. Rodríguez Torronteras, M.D. Ruiz González, L. Izquierdo Palomares, D. Bonilla Valverde, J. Ruiz Laguna, A. Delgado Rubio, J. López-Barea, The β-glucosidase assay: a new diagnostic tool for necrotizing enterocolitis. Sensitivity, specificity, and predictive values, Eur. J. Pediatr. 175 (2016) 931–941, https://doi.org/10.1007/s00431-016-2724-8.
[10] J. Patel, H. Chaudhary, K. Rajput, B. Parekh, R. Joshi, Assessment of gut microbial β-glucuronidase and β-glucosidase activity in women with polycystic ovary syndrome, Sci. Rep. 13 (2023) 1–8, https://doi.org/10.1038/s41598-023-39168-5.
[11] B. Yao, J. Zhao, S. Ding, M.C. Giel, G. Zhang, D. Ding, Y. Tang, Z.H. Weng, Y. Hong, A novel red-emitting aggregation-induced emission probe for determination of β-glucosidase activity, Biomaterials 295 (2023) 122046, https://doi.org/10.1016/j.biomaterials.2023.122046.
[12] J. Liu, H. Bao, C. Liu, F. Wu, F. Gao, "Turn-on" fluorescence determination of β-glucosidase activity using fluorescent polymer nanoparticles formed from Polyethylenimine cross-linked with hydroquinone, ACS Appl. Polym. Mater. 1 (2019) 3057–3063, https://doi.org/10.1021/acsapm.9b00728.
[13] Y. Alacid, M.J. Martínez-Tomé, C.R. Mateo, Reusable fluorescent Nanobiosensor integrated in a multiwell plate for screening and quantification of antidiabetic drugs, ACS Appl. Mater. Interfaces 13 (2021) 25624–25634, https://doi.org/10.1021/acsami.1c02505.
[14] W.Y. Zhang, T. Tian, L.J. Peng, H.Y. Zhou, H. Zhang, H. Chen, F.Q. Yang, A paper-based analytical device integrated with smartphone: fluorescent and colorimetric dual-mode detection of β-glucosidase activity, Biosensors 12 (2022), https://doi.org/10.3390/bios12100893.
[15] G.P. Capozza, M.O. Salazar, I.A. Ramallo, R.L.E. Furlan, Development of a thin-layer chromatography gel-overlay α-glucosidase inhibition assay, J. Planar Chromatogr.–Mod. TLC 36 (2023) 483–491, https://doi.org/10.1007/s00764-023-00279-4.
[16] S. Pandey, A. Sree, S.S. Dash, D.P. Sethi, A novel method for screening beta-glucosidase inhibitors, BMC Microbiol. 13 (2013) 2–6, https://doi.org/10.1186/1471-2180-13-55.
[17] G.Y. Chen, H. Zhang, F.Q. Yang, A simple and portable method for β-glucosidase activity assay and its inhibitor screening based on a personal glucose meter, Anal. Chim. Acta 1142 (2021) 19–27, https://doi.org/10.1016/j.aca.2020.10.047.
[18] N.A. Aschemacher, C.M. Teglia, Á.S. Siano, F.A. Gutierrez, H.C. Goicoechea, Development of an electrochemical sensor using carbon nanotubes and hydrophobic natural deep eutectic solvents for the detection of α-glucosidase activity in extracts of autochthonous medicinal plants, Talanta 268 (2024), https://doi.org/10.1016/j.talanta.2023.125313.
[19] M. Mohiuddin, D. Arbain, A.K.M.S. Islam, M.S. Ahmad, M.N. Ahmad, Alpha-glucosidase enzyme biosensor for the electrochemical measurement of antidiabetic potential of medicinal plants, Nanoscale Res. Lett. 11 (2016) 1–12, https://doi.org/10.1186/s11671-016-1292-1.
[20] J. Li, G. He, B. Wang, L. Shi, T. Gao, G. Li, Fabrication of reusable electrochemical biosensor and its application for the assay of α-glucosidase activity, Anal. Chim. Acta 1026 (2018) 140–146, https://doi.org/10.1016/j.aca.2018.04.015.
[21] Y.C. Boo, Arbutin as a skin depigmenting agent with antimelanogenic and antioxidant properties, Antioxidants 10 (2021) 1129, https://doi.org/10.3390/antiox10071129.
[22] D. Durantel, C. Alotte, F. Zoulim, Glucosidase inhibitors as antiviral agents for hepatitis B and C, Curr. Opin. Investig. Drugs 8 (2007) 125–129.
[23] X. Zhao, Q. Zhang, C.M. Chen, B. Zhang, S. Reiche, A. Wang, T. Zhang, R. Schlögl, D. Sheng Su, Aromatic sulfide, sulfoxide, and sulfone mediated mesoporous carbon monolith for use in supercapacitor, Nano Energy 1 (2012) 624–630, https://doi.org/10.1016/j.nanoen.2012.04.003.
[24] W.Y. Kang, Y.L. Song, L. Zhang, A-Glucosidase inhibitory and antioxidant properties and antidiabetic activity of Hypericum ascyron L, Med. Chem. Res. 20 (2011) 809–816, https://doi.org/10.1007/s00044-010-9391-5.
[25] K. Li, F. Yao, Q. Xue, H. Fan, L. Yang, X. Li, L. Sun, Y. Liu, Inhibitory effects against α-glucosidase and α-amylase of the flavonoids-rich extract from Scutellaria baicalensis shoots and interpretation of structure–activity relationship of its eight flavonoids by a refined assign-score method, Chem. Cent. J. 12 (2018) 1–11, https://doi.org/10.1186/s13065-018-0445-y.
[26] U. Etxeberria, A.L. de la Garza, J. Campión, J.A. Martínez, F.I. Milagro, Antidiabetic effects of natural plant extracts via inhibition of carbohydrate hydrolysis enzymes with emphasis on pancreatic alpha amylase, Expert Opin. Ther. Targets 16 (2012) 269–297, https://doi.org/10.1517/14728222.2012.664134.
[27] K.K. Yadav, S. Paul, Unfolding and refolding study of a large dimeric protein β-glucosidase from almond monitored by fluorescence spectroscopy, Protein Pept. Lett. 22 (2015) 601–610, https://doi.org/10.2174/0929866522666150511151818.
[28] L.V. Chepeleva, O.O. Demidov, A.D. Snizhko, D.O. Tarasenko, A.Y. Chumak, O. O. Kolomoitsev, V.M. Kotliar, E.S. Gladkov, A. Kyrychenko, A.D. Roshal, Binding interactions of hydrophobically-modified flavonols with β-glucosidase: fluorescence spectroscopy and molecular modelling study, RSC Adv. 13 (2023) 34107–34121, https://doi.org/10.1039/d3ra06276g.
[29] T. Arakawa, D. Ejima, T. Akuta, Protein aggregation under high concentration/density state during chromatographic and ultrafiltration processes, Int. J. Biol. Macromol. 95 (2017) 1153–1158, https://doi.org/10.1016/j.ijbiomac.2016.11.005.
[30] J.R. Lakowicz, Fluorescence Anisotropy, in: J.R. Lakowicz (Ed.), Princ. Fluoresc. Spectrosc, Springer US, Boston, MA, 2006, pp. 353–382, https://doi.org/10.1007/978-0-387-46312-4_10.
[31] M.J. Sáenz-Espinar, S. Hafed-Khatiri, D. Salinas-Torres, F. Montilla, F. Huerta, Design of an Electrochemical Device for the detection of alkaline phosphatase inhibitors in seawater, ChemElectroChem 11 (2024) e202400271, https://doi.org/10.1002/celc.202400271.
[32] I. Pastor, M.L. Ferrer, M.P. Lillo, J. Gómez, C.R. Mateo, Structure and dynamics of lysozyme encapsulated in a silica sol−gel matrix, J. Phys. Chem. B 111 (2007) 11603–11610, https://doi.org/10.1021/jp074790b.
[33] I. Pastor, A. Salinas-Castillo, R. Esquembre, R. Mallavia, C.R. Mateo, Multienzymatic system immobilization in sol-gel slides: Fluorescent superoxide biosensors development, Biosens. Bioelectron. 25 (2010) 1526–1529, https://doi.org/10.1016/j.bios.2009.10.029.
[34] M.P. Dale, H.E. Ensley, K. Kern, K.A.R. Sastry, L.D. Byers, Reversible inhibitors of β-glucosidase, Biochemistry 24 (1985) 3530–3539, https://doi.org/10.1021/bi00335a022.
[35] P. Hollander, X. Pi-Sunyer, R.E. Coniff, Acarbose in the treatment of type I, Diabetes Care 20 (1996) 248–253.
[36] A. Tanaka, M. Sugiura, T. Hotta, H. Kurata, Y. Ishihara, Steady-state inhibitory kinetic studies on almond β-glucosidase-catalyzed reaction — binding sites of

monosaccharides, Agric. Biol. Chem. 53 (1989) 1401–1405, https://doi.org/10.1271/bbb1961.53.1401.
[37] A. Tanaka, M. Ito, K. Hiromi, Equilibrium and kinetic studies on the binding of gluconolactone to almond β-glucosidase in the absence and presence of glucose, J. Biochem. 100 (1986) 1379–1385, https://doi.org/10.1093/oxfordjournals.jbchem.a121844.
[38] P. Hollander, X. Pi-Sunyer, R.F. Coniff, Acarbose in the treatment of type I diabetes, Diabetes Care 20 (1997) 248–253, https://doi.org/10.2337/diacare.20.3.248.